ACS Catalysis

pubs.acs.org/acscatalysis

Perspective

Universal Principles for the Rational Design of Single Atom Electrocatalysts? Handle with Care

Giovanni Di Liberto, Luis A. Cipriano, and Gianfranco Pacchioni*

Cite This: *ACS Catal.* 2022, 12, 5846−5856

Read Online

ACCESS | Metrics & More | Article Recommendations | Supporting Information

ABSTRACT: One of the objectives of electronic structure theory is to predict chemical and catalytic activities. This is a challenging target due to the large number of variables that determine the performance of a heterogeneous catalyst. The complexity of the problem has reduced considerably with the advent of single atom catalysts (SACs) and, in particular, of graphene-based SACs for electrocatalytic reactions such as the oxygen reduction (ORR), the oxygen evolution (OER), and the hydrogen evolution (HER) reactions. In this context we assist with a rapidly growing number of theoretical studies based on density functional theory (DFT) and with proposals of universal descriptors that should provide a guide to the experimentalist for the synthesis of efficient catalysts. In this Perspective we critically analyze some of the current problems connected with the prediction of the activity of SACs: accuracy of the calculations, neglect of important contributions in the models used, physical meaning of the proposed descriptors, not to mention some problems of reproducibility. It follows that the "rational design" of a catalyst based on some of the proposed universal descriptors should be considered with caution.

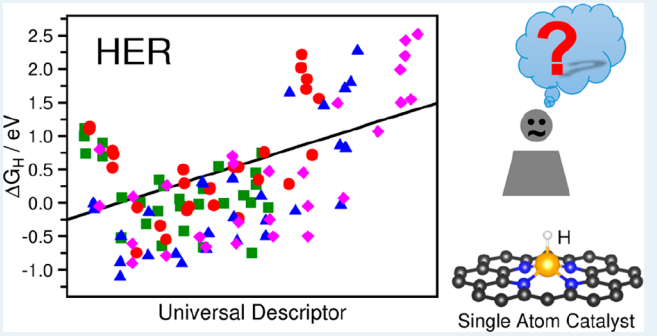

KEYWORDS: *hydrogen evolution reaction, descriptor, volcano plot, density functional theory, single atom catalyst, electrocatalysis, reproducibility*

1. INTRODUCTION

The explosion of studies on single atom catalysts (SACs),[1−3] including several theoretical/computational studies, has stimulated the search for some guiding principles that can help in rationalizing the synthesis of new compounds and explaining the behavior of existing systems.[4] In particular, it is desirable to be able to identify universal descriptors to predict the behavior of SACs in a given reaction or, when this is not possible, to find correlations with meaningful physical parameters for a given subset of SACs.

In the last 3−4 years, several contributions appeared in the literature where correlations or descriptors have been proposed for electrocatalytic reactions such as the oxygen reduction (ORR), the oxygen evolution (OER), and the hydrogen evolution (HER) reactions, or N_2 and CO_2 reduction.[5−16] Sometimes these descriptors correspond to a specific physical property of a SAC, such as the electronegativity of the transition metal center, number of d electrons, position of the d states with respect to the vacuum level, computed charge of the metal atom, electronegativity of neighboring atoms, energy position of bonding or antibonding combinations, etc. However, a simple direct correlation with just one of these variables for a representative number of cases is missing. In the work reported so far, combinations of variables are considered, giving rise to more or less complex expressions in the attempt to identify a single descriptor.

The underlying idea of these studies is to provide a computational basis to screen potential electrocatalysts for one of the reactions mentioned above in order to reduce the experimental burden related to the synthesis and the catalytic tests of new SACs. This process is extremely useful and important, provided that the indications arising from the computational studies are clear, transparent, reliable, and possibly based on descriptors that have their roots in fundamental physical observables.

One important aspect underlying any computational prediction of catalytic activity is the level of reliability of the method and, even more, of the models used to reach the conclusions. Calculations can be trusted if the approximations made and the contributions neglected are not so relevant to invalidate the conclusions. So far, the majority of the calculations reported to identify the existence of universal

Received: February 27, 2022
Revised: April 1, 2022
Published: May 2, 2022

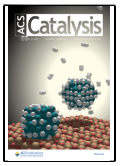

descriptors of SACs in electrocatalysis are based on density functional theory (DFT). However, there are several variants of DFT, each providing a different level of accuracy and reliability, in particular when the quantity of interest is the interaction energy between two units.[17]

The prediction of the activity of a new hypothetical electrocatalyst is usually based on the calculation of the ΔG of adsorption of a given atomic or molecular fragment (e.g., the H atom adsorption energy in the case of the HER). When the ΔG is close to a given value, then the catalyst is expected to be active; otherwise, it is inactive.[18] However, differences in ΔG values of ± 0.2 eV, the typical accuracy of a calculation, can result in radically different measured activities in experiments. Of course, even when a catalyst is expected to be particularly active according to DFT estimates, there are currently no tools to predict whether the synthesis of the new catalyst is accessible or not.

One of the first and most cited examples of universal correlations of SACs in electrocatalysis was reported by Xu et al. in 2018.[5] In this work the authors presented a universal design principle to evaluate the activity of graphene-based SACs toward the ORR, OER, and HER and concluded that the activity is highly correlated with the local environment of the metal center, in particular with its coordination number and electronegativity and with the electronegativity of the nearest-neighbor atoms. Using a relatively simple equation, they were able to plot in a single graph the free energy of adsorption of OH or H fragments for a large series of SACs and to predict their behavior with an analytical function.[5] The most remarkable result is that for a wide series of graphene-based catalysts the computed activities lie along the straight lines defined by the equation, with no exception. The importance of a similar message is apparent: the activity of a SAC can be estimated without performing any simulation.

Since the publication of Xu et al.,[5] other computational studies have been reported on this subject, and often on the same systems, and other expressions for a descriptor have been proposed.[6−11,19,20] These studies have been performed with computational setups similar, although not identical, to that reported by Xu et al.[5] This resulted in a rich database that can be used to further validate (or invalidate) the universal principles introduced by Xu et al.[5] and by others.

In this Perspective article we will critically reconsider the problem. We will show that the identification of universal descriptors for the activity of SACs in electrocatalysis is not as simple as it is often assumed. We will focus on the HER process, both for its importance but also for its relative simplicity, but the conclusions apply to any kind of reaction based on SACs.

The article is organized as follows. In section 2.1 we will compare the results obtained by Xu et al.[5] for a subset of 12 SACs (transition metal (TM) atoms stabilized in N-doped graphene) with recent results from the literature and new calculations done by us for this purpose using the computer code VASP;[21] while there is a general agreement among the literature data and our new set, the results differ substantially from those of Xu et al.[5] obtained with a partly different computational setup. Therefore, in section 2.2 we discuss analytically all the "ingredients" of a DFT calculation to identify the possible sources of the observed discrepancies, identifying in the use of the DFT+U approach (and in general of self-interaction corrected functionals) one of the potential reasons for the different conclusions. In section 2.3 a set of 24 SACs (TM atoms bound to N-doped graphene and to a carbon double vacancy in graphene) has been recomputed at the DFT+U level using the same setup of Xu et al.[5] However, also the new DFT+U results differ substantially from those of ref 5. Possible reasons for this discrepancy are analyzed, and the universal descriptor proposed is questioned. In section 3 a general discussion of the inherent uncertainties in the DFT calculation of adsorption free energies and of the proposed universal descriptors is presented. The final message is that the problem of finding one or more universal descriptors that provide physical insight into the activity of SACs in the HER remains open.

2. RESULTS AND DISCUSSION

2.1. HER on TM@4N-Gr Revisited. Initially we will restrict the analysis to a specific catalyst, nitrogen-doped graphene where a C divacancy has been created, four C atoms are replaced by four N atoms, and a TM atom is stabilized in this coordination mode reminiscent of a pyridinic coordination, TM@4N-Gr (Figure 1(a)). The analysis includes first row TM atoms from Sc to Zn with the addition of Pd and Pt, for a total of 12 SACs.

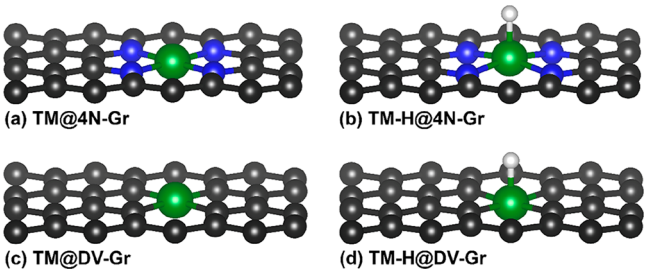

Figure 1. Side views of (a) TM@4N-Gr, (b) TM-H@4N-Gr, (c) TM@DV-Gr, and (d) TM-H@DV-Gr. Rectangular cell.

According to a model proposed by Nørskov and co-workers in 2005,[18] the activity of a catalyst in the HER can be predicted by computing the adsorption energy of a single H atom to a metal electrode, ΔE_H, and determining the corresponding free energy, ΔG_H.[18] If ΔG_H is close to zero, then the system is a potentially good catalyst with a small (ideally zero) overpotential. The idea behind this model is that $\Delta G_H = 0$ eV corresponds to the top of a volcano plot, where the catalyst binds hydrogen neither too strongly nor too weakly. On the contrary, a large positive or negative ΔG_H indicates a poor catalyst due to too weak or too strong bonding with hydrogen, respectively. This model has been improved over the years[22] but, due to its simplicity, is still widely used in the original formulation. It should be mentioned, however, that the model has been introduced for metal surfaces, and its use for SACs may be questionable due to the possible formation of another stable intermediate where two H atoms, and not only one, can bind to the active center (see section 3).[23] Nevertheless, here we concentrate on the hypothesis that the reaction proceeds with formation of a single TM-H intermediate, the condition that has been used so far.[5−11] The ΔG_H values are obtained from ΔE_H by adding a zero-point energy (ZPE) and an entropy term that can be approximated in the same way for all systems; this results in a correction of 0.24 eV ($\Delta G_H = \Delta E_H + 0.24$ eV).

https://doi.org/10.1021/acscatal.2c01011
ACS Catal. 2022, 12, 5846−5856

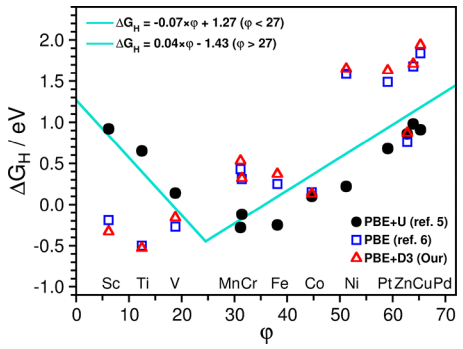

Figure 2. Adsorption free energy of H versus the descriptor φ for single TM atoms supported on N-doped graphene (TM@4N-Gr). This work: PBE+D3, red triangle; Fung et al.:[6] PBE, blue square; Xu et al.:[5] PBE+U, black dot. The connecting line is drawn using eqs 2 and 3. Data taken from Xu, H.; Cheng, D.; Cao, D.; Zeng, X. C. A universal principle for a rational design of single atom electrocatalysts. *Nature Catal.* **2018**, *1*, 339−348. Copyright 2018 Springer Nature; Fung, V.; Hu, G.; Wu, Z.; Jiang, D. E. Descriptors for hydrogen evolution on single atom catalysts in nitrogen-doped graphene. *J. Phys. Chem. C* **2020**, *124*, 19571−19578. Copyright 2020 American Chemical Society.

In Figure 2 we have plotted the original data of Xu et al.,[5] (taken from Table S5 of the Supporting Information), versus the descriptor proposed:

$$\varphi = \theta_d \frac{E_M + \alpha(n_N E_N + n_C E_C)}{E_{O/H}} \quad (1)$$

where E_N and E_C represent the electronegativity of nitrogen and carbon elements, n_N and n_C are the number of nearest-neighbor N and C atoms, and α is a correction coefficient set to 1.25 for single TM-pyrrole-N4 coordination and to 1 for all the other systems. θ_d and E_M correspond to the valence electrons in the d orbital and to the electronegativity of TM atoms. Xu et al.[5] found that the φ descriptor follows a linear relationship when plotted vs the free energy, eqs 2 and 3, with a discontinuity around φ = 27 (see Figure 2):

$$\Delta G_H = -0.07\varphi + 1.27 \ (\varphi < 27) \quad (2)$$

$$\Delta G_H = 0.04\varphi - 1.43 \ (\varphi > 27) \quad (3)$$

In Figure 2 we also reported two additional sets of data (see Table 1). One is taken from a recent work of Fung et al.,[6] while the second is from our group. The three set of results have been obtained with a partly different computational setup but with the same computer code, VASP. In particular, our results are at the PBE+D3 level (D3 = dispersion interactions included),[24] the results of Fung et al.[6] are at the PBE level, while the original data of Xu et al.[5] have been obtained at the PBE+U level.

The PBE (Fung et al.[6]) and the PBE+D3 (present work) values are in close agreement (Table 1 and Figure 2). This is true also if one takes into consideration other recent studies on the same systems[11,19,20] (see Table 1). The common aspect of all these results is that they have been obtained at the PBE level. On the contrary, the PBE+U data by Xu et al.[5] show large deviations (Table 1 and Figure 2). The differences are substantial, with discrepancies of up to 1.5 eV for the cases of Ni, Sc, and Ti. In some cases, the ΔG_H values have different signs: while for Sc and Ti the reaction is predicted to be exergonic at the PBE level, it is endergonic in the results of Xu et al.[5] The distribution of the values obtained at the PBE level is totally different and does not follow the universal behavior proposed by Xu et al.[5] (Figure 2). This opens a serious question about the generality of the universal behavior proposed and the methods required to compute the activity of SACs in electrocatalysis. In an attempt to solve the issue, in the following section we will analyze in detail potential sources of discrepancies between different sets of DFT calculations.

2.2. Effect of Computational Parameters on ΔG_H.

Several parameters need to be considered to reproduce quantitatively a DFT calculation. Often, some of these parameters are assumed to be of little relevance and are not specified in the original papers. In this section we analyze in detail the role of these aspects. The attention is on two specific TM atoms in 4N-Gr, Mn, and Ni which can be considered as representative cases for the HER. The parameters considered are plane wave cutoff and convergence thresholds, number of

Table 1. Adsorption Free Energy ΔG_H (eV) of H on TM in N-Doped Graphene (TM@4N-Gr): PBE and PBE+U Results

	DFT					DFT+U		
	PBE+D3	PBE	PBE	vdw-DF2-c0	PBE+D2	PBE+U	U	Φ
	This work[a]	Fung et al.[b]	Hossain et al[c]	Baby et al.[d]	Zhou et al.[e]	Xu et al.[f]	eV[g]	
Sc@4N-Gr	−0.33	−0.19				0.92	2.11	6.15
Ti@4N-Gr	−0.53	−0.50	−0.92			0.65	2.58	12.45
V@4N-Gr	−0.16	−0.27	−0.28			0.14	2.72	18.80
Cr@4N-Gr	0.32	0.31	0.28			−0.12	2.79	31.41
Mn@4N-Gr	0.53	0.43	0.46			−0.28	3.06	31.16
Fe@4N-Gr	0.37	0.25	0.24	0.19	0.26	−0.25	3.29	38.15
Co@4N-Gr	0.13	0.15	0.13	0.12	0.10	0.10	3.42	44.67
Ni@4N-Gr	1.65	1.59	1.62	1.67	1.58	0.22	3.40	51.20
Cu@4N-Gr	1.71	1.68		1.75	1.45	0.98	3.87	63.91
Zn@4N-Gr	0.87	0.76				0.86	4.12	62.77
Pd@4N-Gr	1.94	1.84	1.86		1.82	0.91		65.27
Pt@4N-Gr	1.63	1.49				0.68		59.07

[a]This work: Spin-polarized calculations done at the PBE+D3 level using the code VASP, hexagonal cell, position of all atoms optimized keeping lattice constant fixed, pseudopotential recommended by VASP, cutoff 400 eV; the truncation criteria for electronic and ionic loops were set to 1×10^{-5} eV and -1×10^{-2} eV/Å, respectively. A $5 \times 5 \times 1$ Monkhorst−Pack k-point grid was used. [b]Reference 6. [c]Reference 11. [d]Reference 19. [e]Reference 20. [f]Reference 5. [g]See text.

https://doi.org/10.1021/acscatal.2c01011
ACS Catal. 2022, 12, 5846−5856

k-points, pseudopotential, dispersion, spin polarization, supercell used and optimization of cell parameters, supercell size (coverage effect), and exchange-correlation functional (comparing the PBE,[25] PBEsol,[26] PBE+U,[27,28] PBE0,[29] and HSE06[30] functionals).

The first two parameters considered, the cutoff of the plane wave basis set (Table S1) and the convergence criteria (Table S2), have virtually no effect as the H adsorption energy remains the same with changes of at most 20 meV.

The effect of the number of k-point grids has been considered by performing the calculations at the Γ point or using a finer grid (Table S3). Since the supercells used are not particularly large, 32 atoms, an effect on ΔG_H is found for Ni@4N-Gr (0.17 eV) when the calculations are done at the Γ point while the use of 5 × 5 × 1 or 10 × 10 × 1 grids does not lead to any further change.

In a similar way, the choice of the pseudopotential used to represent the core electrons of the TM atom is not crucial. One can adopt a small or a large core pseudopotential; the difference is that the $3p^6$ electrons of the TM atom are treated explicitly (small core) or are included in the effective core potential (large core). For all atoms considered in this work we used the pseudopotentials recommended by the VASP manual (sometimes these correspond to a small core, sometimes to large core pseudopotentials).[31] However, the results of Table S4 clearly show that for Mn and Ni the differences are negligible, 30 meV at most.

Next, we considered the role of dispersion, using the Grimme correction in the D3 formulation.[24] Here we observe some change (Table S5) between ΔG_H computed with and without dispersion, but this is always below 60 meV. Notice that the inclusion of dispersion does not necessarily increase the H adsorption energy (Table S5). This can be explained with the fact that dispersion forces act also on the atoms of the support, reinforcing their interactions. The adsorption of an H atom can lead to local distortions with an impact on the stability of the support and can result in small oscillations in the binding energy. Not surprisingly the dispersion contribution to the H atom adsorption is negligible.

An important aspect that is often poorly discussed in theoretical studies (including those on SACs) is the approach followed to represent the support. For the specific case of 4N-Gr, one can cut a hexagonal or a rectangular cell from graphene; the number of atoms is the same, 32, but the way the catalytic center is replicated in space is slightly different. A hexagonal cell is used in most studies,[6,11,19,20] while a rectangular cell was adopted by Xu et al.[5] Usually, the calculations are performed by fixing the lattice parameters of the original graphene support and optimizing the atomic positions (lattice constant "from graphene", Table S6). The other possibility is to fully optimize the lattice constants and atomic coordinates of both the reference system, TM@4N-Gr, and the system with the H atom adsorbed, TM-H@4N-Gr (lattice constant "fully optimized", Table S6). This latter procedure has been followed for both hexagonal and rectangular cells. The results, however, show very small changes, up to 20 meV for Mn@4N-Gr and up to 40 meV for Ni@4N-Gr (Table S6). This shows that the choice of using the lattice constants of the graphene support, which is computationally simpler, is justified. The physical reason is that the local defect created by incorporating a TM atom in the graphene lattice induces only local perturbations.

In supercell calculations of reactions at surfaces, coverage plays an important role.[32] This is because adsorption properties depend on the density of adsorbed species. This effect can be evaluated by comparing the results for supercells of different sizes (Table S7). Going from a 4 × 4 to a 5 × 5 and a 6 × 6 supercell, more than doubling the number of atoms, ΔG_H changes at most by 20 meV. This is due to the local nature of the interaction and the small size of the H atom.

The next aspect considered is spin polarization. TM atoms incorporated in a graphene layer can give rise to magnetic ground states. Even when the atom has a completely filled d or s shell, such as Zn, the addition of a single H atom results in a system with an odd number of electrons. For this reason, the calculations must be performed at the spin-polarized level. A non-spin-polarized calculation describes an unphysical situation. To show this, we have compared spin-polarized and non-spin-polarized calculations for the cases of Mn and Ni (Table S8). Not surprisingly, the effect can be significant. Mn@4N-Gr is predicted to have completely different reactivities if the H adsorption is computed with or without spin polarization, with ΔG_H that goes from 0.45 eV to −0.34 eV, respectively (Table S8). This is because in the ground state of Mn@4N-Gr there are three unpaired electrons mainly localized on the Mn 3d orbitals which reduce to two after H adsorption. For Ni, on the contrary, the difference between the spin-polarized and non-spin-polarized calculations is very small, from 1.65 to 1.69 eV (Table S8). This can be rationalized with the fact that the ground state of Ni@4N-Gr is a singlet closed shell; the addition of a H atom results in an unpaired electron which is partly delocalized, thus explaining the similar results obtained with the two approaches. Spin polarization is essential and indeed has been used in all the studies reported to study this problem.

The last aspect analyzed is probably also the most important one and is related to the choice of the exchange-correlation functional. This has been widely discussed in the literature but not so much for the specific case of SACs. While in the field of semiconductors and insulators it is common to use self-interaction corrected functionals, either hybrid functionals[33,34] or DFT+U,[35] in the field of catalysis by SACs the choice is almost exclusively concentrated on the popular PBE functional, which is not corrected for the self-interaction. The problem has been addressed in a recent study by Patel et al.[36] showing the importance of using hybrid functionals to obtain more reliable results on SACs. In particular, when dealing with systems with localized unpaired electrons it is useful to check that the results are not strongly dependent on the functional used. In Table 2 we have considered ΔG_H for Mn@4N-Gr and Ni@4N-Gr

Table 2. Effect of Exchange-Correlation Functional[a]

ΔG_H (eV)	PBE	PBEsol	PBE+U	PBE0	HSE06
Mn@4N-Gr	0.45 (0.45)	0.32 (0.31)	0.97 (0.97)	1.00	1.01
Ni@4N-Gr	1.72 (1.65)	1.60 (1.52)	1.70 (1.69)	1.73	1.73

[a]Calculations were done with graphene lattice parameters, the position of all atoms optimized, cutoff 450 eV, and pseudopotential recommended by VASP (LC Mn, SC Ni); the truncation criteria for electronic and ionic loops were set to 1×10^{-5} eV and -5×10^{-2} eV/Å, respectively. A 2 × 2 × 1 Monkhorst−Pack k-point grid was used. Values in parentheses were obtained with a 5 × 5 × 1 Monkhorst−Pack k-point grid.

https://doi.org/10.1021/acscatal.2c01011
ACS Catal. 2022, 12, 5846−5856

Table 3. Adsorption Free Energy ΔG_H (eV) of H on a TM in N-Doped Graphene (TM@4N-Gr) and a Double C-Vacancy of Graphene (TM@DV-Gr): PBE+U Results

	This work[a]	Xu et al.[b]	φ		This work[a]	Xu et al.[b]	φ	U, eV[c]
Sc@4N-Gr	−0.28	0.92	6.15	Sc@DV-Gr	0.92	0.86	5.25	2.11
Ti@4N-Gr	−0.33	0.65	12.45	Ti@DV-Gr	0.66	0.46	10.67	2.58
V@4N-Gr	0.18	0.14	18.80	V@DV-Gr	0.80	0.24	16.13	2.72
Cr@4N-Gr	0.71	−0.12	31.41	Cr@DV-Gr	0.78	−0.49	26.95	2.79
Mn@4N-Gr	0.98	−0.28	31.16	Mn@DV-Gr	1.16	−0.53	26.70	3.06
Fe@4N-Gr	0.96	−0.25	38.15	Fe@DV-Gr	1.12	−0.28	32.81	3.29
Co@4N-Gr	0.61	0.10	44.67	Co@DV-Gr	0.83	0.22	38.44	3.42
Ni@4N-Gr	1.73	0.22	51.20	Ni@DV-Gr	0.45	0.31	44.07	3.40
Cu@4N-Gr	1.93	0.98	63.91	Cu@DV-Gr	1.83	0.67	55.00	3.87
Zn@4N-Gr	1.03	0.86	62.77	Zn@DV-Gr	2.02	0.52	53.86	4.12
Pd@4N-Gr	1.80	0.91	65.27	Pd@DV-Gr	0.45	0.75	56.36	—
Pt@4N-Gr	1.45	0.68	59.07	Pt@DV-Gr	0.24	0.20	51.05	—

[a]This work: Spin-polarized DFT+U calculations with VASP code, rectangular cell and lattice parameters fully optimized (V = CTE), cutoff 450 eV, and pseudopotential recommended by VASP. The truncation criteria for electronic and ionic loops were set to 1×10^{-5} eV and -5×10^{-2} eV/Å, respectively. A 5 × 5 × 1 Monkhorst−Pack k-point grid was used. [b]Reference 5. [c]For the origin of the U values, see the text.

using five different functionals (the calculations have been performed with a smaller grid of k points due to the high computational burden associated with hybrid functionals). Besides the standard PBE, we have considered the PBEsol functional explicitly derived for solid systems. However, the results are in line with the PBE ones with changes of ≈0.1 eV (Table 2).

Next we considered the PBE+U approach. DFT+U has been introduced in order to mitigate the problem of the self-interaction error. In general, DFT+U is applicable for localized open shell orbitals, such as the d and f orbitals of TM metal elements, as in the case of strongly correlated materials. The use of the DFT+U approach introduces a variable, the U parameter. There is a wide discussion in the literature on how to determine or chose this term,[37] and it is well-known that the results can critically depend on the U value adopted.[38] For insulators or semiconductors, U is selected to better describe the band gap of these systems, a procedure that cannot be applied to graphene. In the paper by Xu et al.[5] U values between about 2 and 4 eV have been used, as reported in the Supporting Information, but no reference or justification for the choice was given.[5] However, from a literature search we found that the same set of U values has been adopted in 2019 by Gong et al.[39] in a study of CO_2 reduction with SACs; also in this case the U values are reported in the Supporting Information,[39] but nothing is said on their origin except that they have been taken from a work of 2017 of Lin et al.[40] on TM atoms stabilized in covalent organic frameworks. Also Lin et al. do not discuss the U values in the main text, and they report them in the Supporting Information, making reference to the work of 1994 of Solovyev, Dederichs, and Anisimov. This is a LDA+U study of TM impurities in rubidium metal, and the U values are given in a figure only for some TM atoms (V, Cr, Mn, Fe, Co, Ni). The origin of the other U values (Sc, Ti, Cu) is unclear. A possibility is that they have been extrapolated from Figures 2 and 3 of ref 41. Indeed, in the Supporting Information we report a set of U values derived in this way from ref 41 (Table S13 and Figure S1). They are very close to those used in the theoretical studies mentioned above.[5,39,40] This is a typical example of how an important parameter that determines the validity of the results is transferred from paper to paper without a critical assessment of its role and sometimes even without making proper reference to the original source.

Compared to PBE data, the PBE+U results (Table 2) follow the trend found from the analysis of the spin polarization: large effect on Mn and almost no effect on Ni. Once more, this is related to the presence unpaired electrons in Mn@4N-Gr and to the closed shell nature of Ni@4N-Gr. The consequence is that ΔG_H for Mn goes from 0.45 eV (PBE) to 0.97 eV (PBE+U) (Table 2). The difference is not insignificant. In terms of HER activity this means going from a moderately active catalyst to a totally inactive one. On the contrary, no relevant difference is found for Ni where ΔG_H changes by a few millielectronvolts going from PBE to PBE+U (Table 2).

This trend is confirmed when the PBE0 and the HSE06 hybrid functionals are considered (Table 2). The ΔG_H values are very close to the PBE+U ones, with Mn@4N-Gr showing a ΔG_H of about 1 eV and Ni@4N-Gr a ΔG_H of about 1.7 eV (Table 2). The fact that the different behaviors of Mn and Ni are related to the spin distribution is confirmed by the analysis of the spin localization, which is always more pronounced with the self-interaction corrected functionals (see Table S9).

Of all the computational aspects considered, two emerge as being more critical: (a) the necessity to use spin-polarized calculations since TM atoms embedded in graphene may have magnetic ground states and (b) the choice of the exchange-correlation functional. In particular, significant deviations emerge for high spin complexes when comparing standard GGA with self-interaction corrected functionals. This aspect has received relatively little attention so far in the discussion of SACs.

2.3. HER from PBE+U Results: A Critical Analysis. Of the effects considered, not surprisingly the choice of the functional is the most important one. We have seen above that substantially different conclusions are obtained when the activity of SACs in the HER is computed at the PBE[6,11,19,20] or PBE+U levels, as done in the work of Xu et al.[5] (see section 2.1). For this reason, we recomputed a subset of SACs at the PBE+U level in order to compare the results with those obtained with PBE (Table 1) and of ref 5. The same computational setup used by Xu et al.[5] has been adopted; in particular, the lattice constants of TM@4N-Gr and TM-H@4N-Gr have been fully optimized using a rectangular cell (see

https://doi.org/10.1021/acscatal.2c01011
ACS Catal. 2022, 12, 5846−5856

Tables S10 and S11). The computed ΔG_H values are reported in Table 3.

First of all, comparing Table 1 (PBE, this work) and Table 3 (PBE+U, this work), it appears that for several atoms the results are similar (see e.g. Sc, Ti, Ni, Cu, Zn, Pd, Pt). The effect of the U parameter is large for the atoms at the center of the first row of TM atoms, i.e. for V, Cr, Mn, Fe, and Co. However, the difference of ΔG_H(PBE) and ΔG_H(PBE+U) is always below 0.6 eV.

In Table 3, our PBE+U results are compared with those of Xu et al.[5] With the exception of V@4N-Gr, there is a large discrepancy between the two sets of data. The differences are substantial, often of the order of 1 eV or more. For Sc@4N-Gr we compute a ΔG_H of −0.28 eV against a reported value of +0.92 eV; particularly relevant is the discrepancy found for Ni@4N-Gr, where our value is 1.73 eV while that reported by Xu et al.[5] is 0.22 eV. In terms of HER activity this means going from a dead catalyst to a highly efficient one.

An effect not considered so far is that of strain in the 4N-Gr support. To examine this contribution, we have introduced tensile and compressive strains on the graphene cell. This is done by expanding or compressing the graphene lattice parameters by −2%, + 2%, and +4% in both crystallographic directions, *a* and *b*. In this way a uniform strain is introduced in the film. ΔG_H has then been computed as a function of strain for the two prototypical elements, Mn and Ni (Table S12).

For Mn@4N-Gr a ±2% strain, compressive or tensile, has a moderate effect on ΔG_H, <0.2 eV (Table S12). With a strain of +4%, ΔG_H goes from 0.97 to 1.50 eV (Table S12). The effect is large also on Ni@4N-Gr but goes in the opposite direction. A compressive strain of −2% results in an increase of ΔG_H from 1.69 to 1.92 eV; a tensile strain results in a decrease of ΔG_H (from 1.69 to 1.11 eV for a + 4% strain). In a personal communication,[42] the authors of ref 5 mentioned that their calculations on Ni@4N-Gr were done using the following cell parameters: *a* = 8.77 Å, *b* = 10.17 Å (Ni@4N-Gr), *a* = 8.66 Å, *b* = 10.10 Å (Ni-H@4N-Gr). Indeed, with these values we compute a ΔG_H of 0.32 eV, close to that reported in the original paper (0.22 eV).[5] However, these lattice constants are significantly strained compared to our optimized values: *a* = 8.38 Å, *b* = 9.95 Å (Ni@4N-Gr), *a* = 8.40 Å, *b* = 10.00 Å (Ni-H@4N-Gr). This corresponds to a 3−5% strain along the *a* direction and almost no strain along the *b* direction (0−2%). With these strained lattice constants, the total energies of the Ni@4N-Gr and Ni−H@4N-Gr systems are 2.42 and 0.76 eV, respectively, higher than the minimum structures. Since the strained reference structure, Ni@4N-Gr, is destabilized by 1.66 eV more than the H complex, this explains the higher reactivity found toward hydrogen (small ΔG_H). However, the reasons why the supports used by Xu et al.[5] are strained and how the strain has been determined remain unclear.

The conclusion is that for the 12 SACs with N-doped graphene structure, large discrepancies exist between the two sets of PBE+U data. To check if this is restricted to the specific SACs considered, the analysis has been extended to 12 SACs where the same TM atoms, from Sc to Zn, Pd, and Pt, are embedded in a carbon double vacancy in graphene (TM@DV-Gr) (Figure 1(c and d) and Table 3). In this model the TM atom is directly bound to four C atoms, and the chemical environment is totally different from that of 4N-Gr; therefore, also the values of the descriptor φ are different.

The general conclusions, however, are the same as for the 12 N-doped graphene SACs (TM@4N-Gr). Large discrepancies exist between the presently computed values and the ΔG_H values of ref 5. For instance, for Cr@DV-Gr, Mn@DV-Gr, and Fe@DV-Gr we found large positive ΔG_H values of 0.8−1.2 eV, while Xu et al.[5] reported negative free energies of −0.3/−0.5 eV (Table 3). The only systems where the two set of data agree are Sc@DV-Gr, Ti@DV-Gr, Ni@DV-Gr, and Pt@DV-Gr. The consequence is that the data points do not follow the universal rule proposed but are rather scattered (Figure 3).

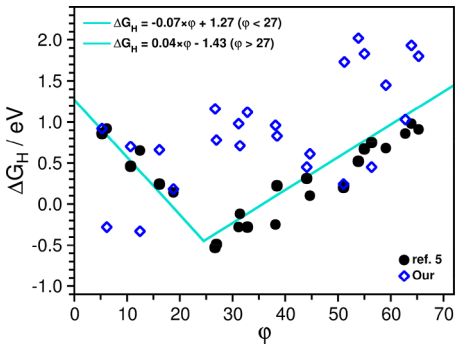

Figure 3. Adsorption free energies of H (PBE+U results) versus the descriptor φ for single TM atoms supported on N-doped graphene (TM@4N-Gr) and on a carbon double vacancy in graphene (TM@DV-Gr). This work: blue diamonds; Xu et al.:[5] black dots. The connecting line is drawn using eqs 2 and 3. Data taken from Xu, H.; Cheng, D.; Cao, D.; Zeng, X. C. A universal principle for a rational design of single atom electrocatalysts. *Nature Catal.* **2018**, *1*, 339−348. Copyright 2018 Springer Nature.

To summarize, analyzing the performances of 24 models of SACs in the HER, conflicting conclusions emerge from the analysis of data reported in the literature. In particular, significant differences exist between some recent reports[6,11,19,20] and the data reported by Xu et al.[5] For this subset of SACs the nice universal principle underlying the reactivity of SACs proposed in ref 5 cannot be confirmed. The computed free energies for H adsorption plotted versus the universal descriptor proposed (eq 1) do not show the behavior reported in the original paper (Figure 3). Furthermore, of the 24 cases examined, the data of Xu et al.[5] are reproducible only in 5−6 cases. This is an important warning since the data set reported in ref 5 is being used as training set for machine learning screening of SACs.[6,43] The authors of ref 5 and the Journal have been informed.

3. DFT MODELING OF SACS IN THE HER: A CRITICAL VIEW

The field of theoretical modeling of SACs for electrocatalysis is growing very rapidly, with several new contributions appearing every week. This is largely due to the relatively simple nature of SACs, in particular when based on graphene structures. Differently from SACs stabilized on metal or oxide surfaces, a single layer of graphene can be modeled with small supercells. Furthermore, with respect to more complex reactions, the study of the ORR, OER, and HER does not require consideration of complex adsorbed species and several isomers on the surface of the catalyst. A screening of the reactivity can be done with simple models where the key parameters are the adsorption free energies of some molecular fragments.[18] The HER case is also the simplest, since here it is sufficient to adsorb a single H atom and compute the adsorption energy to predict the activity of a SAC. This

https://doi.org/10.1021/acscatal.2c01011
ACS Catal. 2022, 12, 5846−5856

explains the large number of hypothetical catalysts (hundreds and sometimes thousands) that have been tested. However, this also raises a fundamental question for the experimentalist: to what extent can these calculations be trusted? We have seen cases where the results lead to conflicting conclusions. In this section we will try to provide an answer to this question by considering some aspects that are often underestimated in the discussion of the problem.

3.1. Exchange-Correlation Functional. A general problem, largely ignored in the discussion on this topic, is the role of the exchange-correlation functional. The majority of studies performed on graphene-based SACs in the HER are done at the GGA level (e.g., using the PBE functional).[6−16,19,20] It is well-known that the calculation of binding energies is probably the most delicate aspect of modern DFT. In fact, depending on the functional used, significant oscillations can be found in the stability of a molecular complex. To establish an error bar on this quantity is difficult, as this is largely system and method dependent. Considering the examples analyzed in this work, we can conclude that the oscillations can go up to 0.7 eV (Table 2). This is a huge quantity when one aims at predicting the expected overpotential for the HER. It is the difference between a promising and a totally inert catalyst. Of course, some exchange-correlation functionals are more accurate than others in describing the physics of the process and its energetics. When localized unpaired electrons are involved, which is the case of several TM atoms stabilized in a carbon matrix, the use of hybrid functionals is better justified.[36] In this respect, benchmark calculations with highly accurate quantum-chemical approaches (coupled cluster) are highly needed in order to assess the reliability of the computed values. In general, the fact that ΔG_H may depend significantly on the method used should suggest some caution in predicting the activity of single atoms in electrocatalysis.

3.2. Details of the Calculation. In every DFT calculation some parameters need to be defined: plane waves cutoff, convergence criteria, size of the supercells, number of k points, choice of the pseudopotential, inclusion of dispersion, level of optimization, etc. Each of these terms has a small but non-negligible effect, of the order of 20−50 meV. One can hope that contributions of opposite sign will lead to a cancellation of error, but this is not guaranteed. An uncertainty of the order of 0.1 eV, if not more, is unavoidable and inherent in the approach.

3.3. Number of Intermediates and Kinetic Model. The model used to screen the activity of SACs in the HER is an extension of that proposed by Nørskov et al.[18] for metal surfaces. However, there is a fundamental difference between a metal surface and a SAC. SACs are reminiscent of coordination compounds.[44] While on metal surfaces the formation of the MH complex is followed by desorption of $^1/_2H_2$ without formation of other intermediates (with the exception of the physisorbed H_2 molecule, irrelevant for the kinetics), on SACs besides MH intermediates also HMH stable complexes can form where two H atoms are bound to the catalytic center (dihydrogen or dihydride complexes).[23] When this occurs, the kinetics of the process changes, and the simple two-dimensional volcano plot which is at the basis of the original Nørskov model is no longer sufficient, as the reaction implies that both ΔG_H values for the two reaction steps are close to zero, and not just one.[23] Neglecting this second step can lead to completely incorrect conclusions about the activity of a SAC.

3.4. Thermodynamic Stability. SACs are not static objects; they may change their position in the course of the reaction.[45] This opens an important aspect in the theoretical evaluation of the activity of SACs, which is their stability in different environments, such as in oxidizing or reducing conditions. Ab initio thermodynamic analyses of surface phase diagrams provide the conditions of O_2 and H_2 partial pressures and the temperatures at which a given structure is stable, showing that the stability of a given configuration of a SAC is a critical function of the reaction conditions.[46]

3.5. Solvent Effects. All the electrocatalytic reactions we are referring to occur in water, and the solvent can play an important role in stabilizing (or destabilizing) a given surface complex. The presence of a liquid/solid interface may change in a nontrivial way the nature of the catalytic support. The solvent can be included in various ways, through an implicit representation of a continuous dielectric,[47] or as the result of the molecular interaction with explicit water molecules in conjunction with molecular dynamics (MD),[48] in static simulations with a water layer,[49,50] or with microsolvation models.[51] The computational approach chosen has important implications for the H adsorption energy, which can change by up to a few tenths of an electronvolt once the solvent is considered.[52,53] Thus, no matter whether explicit or implicit solvent effects are considered, these can modify the reactivity, leading to quantitatively, and possibly even qualitatively, different predictions. The fact that the majority of the descriptors proposed so far are based on "dry" models of the catalyst implies the assumption that the role of the solvent is negligible, an aspect that needs to be further investigated.

3.6. pH Dependence. HER reactions are pH dependent.[54,55] Nevertheless, it is common practice that the experimentally observed behavior of catalysts for the HER in variable pH conditions is rationalized based on DFT calculations where the pH is not explicitly taken into account.[56,57] The pH contribution to the Gibbs free energy can be included by considering a term of the type $k_bT\ \ln_{(10)}$ pH, as reported by Nørskov and co-workers.[58] While probably this is not the most severe problem, it also contributes to some uncertainty on the computed values.

3.7. Shift in the Volcano Plot. The general model adopted to assess the potential activity of a SAC is based on the condition that ΔG_H is close to zero for zero overpotential η ($\Delta G_H = 0$ eV at $\eta = 0$ V). This corresponds to a catalyst at the top of the volcano plot that binds hydrogen not too strongly or too weakly (Sabatier principle). Recently, this model has been questioned.[59] By linking microkinetics to the free-energy diagrams for the HER, it has been suggested that in the high overpotential regime, $\eta > 0.10$ V, the steady state is a better approximation than the quasi-equilibrium condition. This results in revised volcano curves for the HER which show that the most active electrocatalysts in the HER do not bind hydrogen thermoneutrally but rather stabilize the H intermediate endergonically at zero overpotential. Thus, the best catalytic materials in the HER do not correspond to the condition $\Delta G_H \approx 0$ but to $\Delta G_H \approx 0.2$ once the applied overpotential and kinetics are taken into account in the analysis, as observed experimentally.[60,61] So far, none of the universal descriptors proposed from DFT screening takes this fact into account.

https://doi.org/10.1021/acscatal.2c01011
ACS Catal. 2022, 12, 5846−5856

3.8. Comparison with Experiment. The natural way to validate the results of a DFT calculation is to compare with experiment. SACs are not an exception. For obvious reasons, the results of a DFT calculation can be compared to experiment only when the structure of the SAC is the same as that of the actual catalyst. Even small changes in the coordination can lead to substantially different results.[62,63] A precise definition of the structure of a SAC is challenging. Electron microscopy, X-ray spectroscopies (XANES and EXAFS), high resolution STEM, infrared spectroscopy of adsorbed probe molecules, etc., often in combination and supported by DFT results, can provide an accurate identification of the structure of the catalyst.[64−66] However, in most cases the nature of the SAC is only partly clarified, making a direct comparison with DFT purely tentative. From a careful search of the literature, it turns out that the cases where the nature of a TM incorporated in a graphene-based support is unambiguously identified and the structure elucidated at the atomistic level are scarce.[67−69] Much more common are claims of good agreement for calculated structures that, in principle, could be rather different from the measured ones. When this is the case, the agreement is probably the consequence of a lucky cancellation of errors. Another aspect that is often neglected is the dynamical nature of the catalyst under reaction conditions.[45] In this respect in situ/operando techniques such as X-ray absorption spectroscopy, scanning tunneling microscopy, and Fourier-transform infrared spectroscopy can be extremely valuable to study the evolution of SACs.[70]

3.9. Universal Descriptors. This brief discussion should have clarified that the use of DFT calculations to predict the behavior of SACs in electrocatalysis is more problematic than usually assumed. This contrasts with the growing number of studies where universal descriptors or correlations are proposed, based either on equations of various complexity or on the analysis of large data sets with the help of machine learning techniques.

In some cases, relatively simple relations are proposed, as in the work of Huang et al.[7] where the HER reaction has been studied on SACs consisting of TM atoms stabilized on the surface of MoS_2, WS_2, and ZrS_2. The authors showed that the catalytic performance is highly correlated with the electronegativity of the active site and its neighboring atoms as well as with the distance between them. Here the notion of electronegativity is introduced, a quantity which is not a physical observable but is a very useful concept in chemistry. However, if one tries to extend the model proposed by Hang et al.[7] to the 24 graphene-based systems considered in this Perspective, the points are sparse and the correlation found is not spectacular ($R^2 < 0.8$). This suggests that while simple correlations may be found, these are restricted to a given subset of catalysts (in this respect, they are not universal).

In other studies, more complex formulas have been proposed to identify a descriptor of the behavior of SACs. For instance, Qi et al.[8] introduced a function that depends on the ratio between the product of the number of valence electrons of the n atoms in the catalytic center elevated to $2/n$ and the product of the electronegativities of the same centers elevated to $1/n$. The physical meaning of this equation cannot be clearly identified. Furthermore, in some of the plots reported (see e.g. Figure 4a in ref 8) the H adsorption energy of a few SACs, although available, is not reported. Reducing the number of points, of course, results in a better fit. Sometimes there is simply a certain approximation in reporting the data. In the study of Hossain et al.[11] the ΔG_H values are not given in a table but are plotted in Figure 1 against the reaction pathway and in Figure 2 against the energy of an antibonding orbital. It turns out that ΔG_H for Os@N-Gr is about −0.8 eV in Figure 1 and about +0.8 eV in Figure 2. While this is surely a small mistake, the reader is confused about the thermodynamic balance of the HER for this hypothetical catalyst.

Recently a universal descriptor for the HER on TM dichalcogenides has been proposed where the main physical quantity that enters in the definition is the "bond electronegativity",[9] a not widely used property that has been introduced to rationalize bond strength in superhard materials.[71] The problem with these quantities is that they (1) are not physical observables and (2) must be derived from calculations (e.g., from Bader atomic charges),[72] a procedure not free from limitations and which is method dependent.

Another descriptor that is often used in this context is the d-band center model.[6,73] This successful model has been introduced a long time ago by Hammer et al.[74] to describe the reactivity of metal surfaces where valence electrons occupy wide bands. But SACs consist of isolated TM atoms incorporated in a surrounding environment. The surface acts as a giant ligand, resulting in the split of the five d orbitals of the metal center due to the interaction with the orbitals of the neighboring atoms. Since SACs are by definition isolated, their d levels cannot form a band, and their properties are better described in terms of molecular orbitals. In fact, macrocycle ligands have been used to model the infinite graphene layer.[6] In this respect, the notion of frontier orbitals, widely used in coordination chemistry,[75] is a much more appropriate descriptor than the d-band center. In Figure 4 we report the projected density of states (DOS) for a Ni atom embedded in 4N-Gr and for a Ni(100) surface: it is apparent that the two systems have completely different DOS curves, with largely localized and narrow states for the Ni SAC and broad bands for metallic Ni. It should also be mentioned that the precise evaluation of the position of the d-band center in graphene-based SACs is not trivial, due to strong hybridization of the metal and "ligand" orbitals.

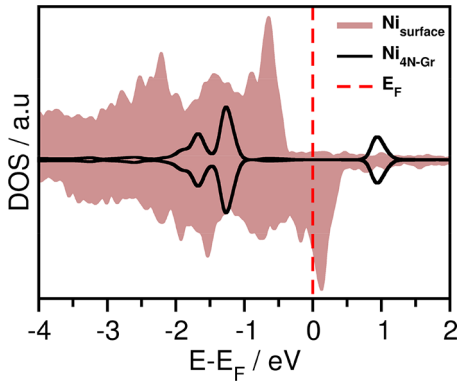

Figure 4. Density of states projected on 3d orbitals for a Ni atom embedded in N-doped graphene, Ni@4N-Gr, and for a Ni(100) surface.

Not surprisingly, given the possibility to produce large sets of data, some authors have resorted to the use of machine learning to extract useful information.[43,76] Statistical learning techniques can improve the search for descriptor-based

https://doi.org/10.1021/acscatal.2c01011
ACS Catal. 2022, 12, 5846−5856

performance equations, but the black-box nature of these methods makes a physical interpretation of the resulting descriptors difficult when not impossible. In a recent study Fung et al.[6] analyzed a set of 3d, 4d, and 5d TM atoms embedded in N-doped graphene. They found that the d-band center correlates very poorly with the ΔG_H values (not surprisingly, see above). Therefore, they introduced ten other descriptors and used a SISSO algorithm (sure independence screening and sparsifying operator) to obtain an expression which is a function of five variables only: the d-band center, the Bader charge, the inverse of the covalent radius, the electronegativity, and the square of the number of occupied d states. Many of these quantities are not rigorously defined, and most of them need to be calculated, which makes again the expression method dependent. While useful in principle to screen new potential catalysts, the complexity of the relation, the number of variables, and the fact that some are not easily defined limit our understanding of the physical reasons that determine the chemical behavior of a given SAC. Nevertheless, useful examples of applications of machine learning techniques exist.[77] Recently an interesting hybrid approach has been proposed for a specific hydrodehalogenation reaction where experimental activity and selectivity are analyzed as a function of only two chemical descriptors from DFT.[77]

4. CONCLUDING REMARKS

We hope we have shown that the H adsorption energy on single atom electrocatalysts is a delicate quantity and that several factors can contribute to the computed values. Screening of large data sets based on incomplete models (no solvent, no inclusion of other intermediates than the MH one) or on exchange-correlation functionals not corrected for the self-interaction, just to mention the most important effects, can lead to uncertain predictions. The effect of these contributions is not the same for different active sites on different supports, and some SACs may be affected more than others. To place an error bar on the accuracy of the computed adsorption free energies is not simple, as once more the error is system dependent, but a prudential estimate is that the computed ΔG_H values have uncertainties that can go from 0.1 to 0.5 eV or more. These are large quantities in terms of overpotential for the reaction. Using predicted activities of new catalysts coming from DFT calculations, these aspects should be considered.

In an era where computing power has increased enormously, perhaps the time has come to shift the attention from the quantity of the data produced to the quality of the predicted behaviors and of the descriptors used to rationalize the chemistry of these systems. This could result in a better understanding of the physical and chemical origins of the catalytic activity and be of real help to the experimentalist in designing new efficient catalytic systems.

ASSOCIATED CONTENT

Supporting Information

The Supporting Information is available free of charge at https://pubs.acs.org/doi/10.1021/acscatal.2c01011.

Effect of computational parameters on the H adsorption free energy; effect of the truncation criteria for electronic and ionic loops; effect of k-point grid; effect of pseudopotential for the TM atom; effect of dispersion; cell parameters; effect of supercell size; effect of spin polarization; orbital occupancy as a function of the exchange-correlation functional; optimized lattice constants; effect of strain; U values for PBE+U calculations; U-J parameter for the 3d group of transition metals (PDF)

AUTHOR INFORMATION

Corresponding Author

Gianfranco Pacchioni − *Dipartimento di Scienza dei Materiali, Università di Milano - Bicocca, 20125 Milano, Italy;* orcid.org/0000-0002-4749-0751; Email: Gianfranco.pacchioni@unimib.it

Authors

Giovanni Di Liberto − *Dipartimento di Scienza dei Materiali, Università di Milano - Bicocca, 20125 Milano, Italy;* orcid.org/0000-0003-4289-2732

Luis A. Cipriano − *Dipartimento di Scienza dei Materiali, Università di Milano - Bicocca, 20125 Milano, Italy;* orcid.org/0000-0002-3801-7751

Complete contact information is available at: https://pubs.acs.org/10.1021/acscatal.2c01011

Author Contributions

The manuscript was written through contributions of all authors.

Notes

The authors declare no competing financial interest.

All inputs and outputs of the DFT calculations reported in the paper can be found on the open repository Bicocca Open Archive Research Data: https://board.unimib.it/datasets/jvwf8v2tgb/1.

ACKNOWLEDGMENTS

We acknowledge the financial support from the Italian Ministry of University and Research (MIUR) through PRIN Project 20179337R7 and the grant Dipartimenti di Eccellenza -2017 “Materials For Energy”. Access to the CINECA supercomputing resources was granted via ISCRAB. We also thank COST Action 18234 supported by COST (European Cooperation in Science and Technology).

REFERENCES

(1) Liu, L.; Corma, A. Confining isolated atoms and clusters in crystalline porous materials for catalysis. *Nature Rev. Mater.* **2021**, *6*, 244−263.

(2) Wang, A.; Li, J.; Zhang, T. Heterogeneous single-atom catalysis. *Nature Rev. Chem.* **2018**, *2*, 65−81.

(3) Lang, R.; Du, X.; Huang, Y.; Jiang, X.; Zhang, Q.; Guo, Y.; Liu, K.; Qiao, B.; Wang, A.; Zhang, T. Single-atom catalysts based on the metal-oxide interaction. *Chem. Rev.* **2020**, *120*, 11986−12043.

(4) Zhao, Z. J.; Liu, S.; Zha, S.; Cheng, D.; Studt, F.; Henkelman, G.; Gong, J. Theory-guided design of catalytic materials using scaling relationships and reactivity descriptors. *Nature Rev. Mater.* **2019**, *4*, 792−804.

(5) Xu, H.; Cheng, D.; Cao, D.; Zeng, X. C. A universal principle for a rational design of single-atom electrocatalysts. *Nature Catal.* **2018**, *1*, 339−348.

(6) Fung, V.; Hu, G.; Wu, Z.; Jiang, D. E. Descriptors for hydrogen evolution on single atom catalysts in nitrogen-doped graphene. *J. Phys. Chem. C* **2020**, *124*, 19571−19578.

(7) Huang, H. C.; Zhao, Y.; Wang, J.; Li, J.; Chen, J.; Fu, Q.; Bu, Y. X.; Cheng, S. B. Rational design of an efficient descriptor for single-

atom catalysts in the hydrogen evolution reaction. *J. Mater. Chem. A* **2020**, *8*, 9202−9208.
(8) Qi, L.; Gao, W.; Jiang, Q. Effective descriptor for designing high-performance catalysts for the hydrogen evolution reaction. *J. Phys. Chem. C* **2020**, *124*, 23134−23142.
(9) Ran, N.; Qiu, W.; Song, E.; Wang, Y.; Zhao, X.; Liu, Z.; Liu, J. Bond electronegativity as hydrogen evolution reaction catalyst descriptor for transition metal (TM= Mo, W) dichalcogenides. *Chem. Mater.* **2020**, *32*, 1224−1234.
(10) Liu, J.; Liu, H.; Chen, H.; Du, X.; Zhang, B.; Hong, Z.; Sun, S.; Wang, W. Progress and challenges toward the rational design of oxygen electrocatalysts based on a descriptor approach. *Adv. Science* **2020**, *7*, 1901614.
(11) Hossain, M. D.; Liu, Z.; Zhuang, M.; Yan, X.; Xu, G. L.; Gadre, C. A.; Hao, Y.; Pan, X.; Amine, K.; Luo, Z. Rational design of graphene-supported single atom catalysts for hydrogen evolution reaction. *Adv. Ener. Mater.* **2019**, *9*, 1803689.
(12) Jovanović, A. Z.; Mentus, S. V.; Skorodumova, N. V.; Pašti, I. A. Reactivity Screening of Single Atoms on Modified Graphene Surface: From Formation and Scaling Relations to Catalytic Activity. *Adv. Mater. Interface* **2021**, *8*, 2001814.
(13) Huang, H. C.; Li, J.; Zhao, Y.; Chen, J.; Bu, Y. X.; Cheng, S. B. Adsorption energy as a promising single-parameter descriptor for single atom catalysis in the oxygen evolution reaction. *J. Mater. Chem. A* **2021**, *9*, 6442−6450.
(14) Yuan, H.; Li, Z.; Zeng, X. C.; Yang, J. Descriptor-based design principle for two-dimensional single-atom catalysts: carbon dioxide electroreduction. *J. Phys. Chem. Letters* **2020**, *11*, 3481−3487.
(15) Nong, W.; Qin, S.; Huang, F.; Liang, H.; Yang, Z.; Qi, C.; Li, Y.; Wang, C. Designing C_3N-supported single atom catalysts for efficient nitrogen reduction based on descriptor of catalytic activity. *Carbon* **2021**, *182*, 297−306.
(16) Talib, S. H.; Lu, Z.; Yu, X.; Ahmad, K.; Bashir, B.; Yang, Z.; Li, J. Theoretical inspection of M1/PMA single-atom electrocatalyst: ultra-high performance for water splitting (HER/OER) and oxygen reduction reactions (OER). *ACS Catal.* **2021**, *11*, 8929−8941.
(17) Sousa, S. F.; Fernandes, P. A.; Ramos, M. J. General performance of density functionals. *J. Phys. Chem. A* **2007**, *111*, 10439−10452.
(18) Nørskov, J. K.; Bligaard, T.; Logadottir, A.; Kitchin, J. R.; Chen, J. G.; Pandelov, S.; Stimming, U. Trends in the Exchange Current for Hydrogen Evolution. *J. Electrochem. Soc.* **2005**, *152* (3), J23.
(19) Baby, A.; Trovato, L.; Di Valentin, C. Single atom catalysts (SAC) trapped in defective and nitrogen-doped graphene supported on metal substrates. *Carbon* **2021**, *174*, 772−788.
(20) Zhou, Y.; Gao, G.; Li, Y.; Chu, W.; Wang, L. W. Transition-metal single atoms in nitrogen-doped graphenes as efficient active centers for water splitting: a theoretical study. *Phys. Chem. Chem. Phys.* **2019**, *21*, 3024−3032.
(21) Kresse, G.; Furthmüller, J. Efficient Iterative Schemes for Ab Initio Total-Energy Calculations Using a Plane-Wave Basis Set. *Phys. Rev. B - Condens. Matter Mater. Phys.* **1996**, *54* (16), 11169−11186.
(22) Exner, K. S. Does a Thermoneutral Electrocatalyst Correspond to the Apex of a Volcano Plot for a Simple Two-Electron Process? *Angew. Chemie Int. Ed.* **2020**, *59*, 10236−10240.
(23) Di Liberto, G.; Cipriano, L. A.; Pacchioni, G. Role of Dihydride and Dihydrogen Complexes in Hydrogen Evolution Reaction on Single-Atom Catalysts. *J. Am. Chem. Soc.* **2021**, *143*, 20431−20441.
(24) Grimme, S.; Antony, J.; Ehrlich, S.; Krieg, H. A Consistent and Accurate Ab Initio Parametrization of Density Functional Dispersion Correction (DFT-D) for the 94 Elements H-Pu. *J. Chem. Phys.* **2010**, *132* (15), 154104.
(25) Perdew, J. P.; Burke, K.; Ernzerhof, M. Generalized Gradient Approximation Made Simple. *Phys. Rev. Lett.* **1996**, *77*, 3865−3868.
(26) Perdew, J. P.; Ruzsinszky, A.; Csonka, G. I.; Vydrov, O. A.; Scuseria, G. E.; Constantin, L. A.; Zhou, X.; Burke, K. Restoring the density-gradient expansion for exchange in solids and surfaces. *Phys. Rev. Lett.* **2008**, *100*, 136406.
(27) Anisimov, V. I.; Zaanen, J.; Andersen, O. K. Band theory and Mott insulators: Hubbard U instead of stoner I. *Phys. Rev. B: Condens. Matter Mater. Phys.* **1991**, *44*, 943.
(28) Dudarev, S.; Botton, G.; Savrasov, S.; Humphreys, C.; Sutton, A. Electron-energy-loss spectra and the structural stability of nickel oxide: An LSDA+U study. *Phys. Rev. B: Condens. Matter Mater. Phys.* **1998**, *57*, 1505.
(29) Adamo, C.; Barone, V. Toward reliable density functional methods without adjustable parameters: The PBE0 model. *J. Chem. Phys.* **1999**, *110*, 6158−6170.
(30) Heyd, J.; Scuseria, G. E.; Ernzerhof, M. Hybrid functionals based on a screened Coulomb potential. *J. Chem. Phys.* **2003**, *118*, 8207−8215.
(31) https://www.vasp.at/documentation/.
(32) Jin, K. H.; Choi, S. M.; Jhi, S. H. Crossover in the adsorption properties of alkali metals on graphene. *Phys. Rev. B* **2010**, *82*, 033414.
(33) Gerosa, M.; Bottani, C. E.; Di Valentin, C.; Onida, G.; Pacchioni, G. Accuracy of dielectric-dependent hybrid functionals in the prediction of optoelectronic properties of metal oxide semiconductors: a comprehensive comparison with many-body GW and experiments. *J. Phys.: Conden. Matter* **2018**, *30*, 044003.
(34) He, J.; Franchini, C. Assessing the performance of self-consistent hybrid functional for band gap calculation in oxide semiconductors. *J. Phys.: Condens. Matter* **2017**, *29*, 454004.
(35) Finazzi, E.; Di Valentin, C.; Pacchioni, G.; Selloni, A. Excess electron states in reduced bulk anatase TiO 2: comparison of standard GGA, GGA+ U, and hybrid DFT calculations. *J. Chem. Phys.* **2008**, *129*, 154113.
(36) Patel, A. M.; Ringe, S.; Siahrostami, S.; Bajdich, M.; Nørskov, J. K.; Kulkarni, A. R. Theoretical approaches to describing the oxygen reduction reaction activity of single-atom catalysts. *J. Phys. Chem. C* **2018**, *122*, 29307−29318.
(37) Cococcioni, M.; De Gironcoli, S. Linear response approach to the calculation of the effective interaction parameters in the LDA+ U method. *Phys. Rev. B* **2005**, *71*, 035105.
(38) Capdevila-Cortada, M.; Łodziana, Z.; López, N. Performance of DFT+ U approaches in the study of catalytic materials. *ACS Catal.* **2016**, *6*, 8370−8379.
(39) Gong, L.; Zhang, D.; Lin, C. Y.; Zhu, Y.; Shen, Y.; Zhang, J.; Han, X.; Zhang, L.; Xia, Z. Catalytic mechanisms and design principles for single-atom catalysts in highly efficient CO2 conversion. *Adv. Ener. Mater.* **2019**, *9*, 1902625.
(40) Lin, C. Y.; Zhang, L.; Zhao, Z.; Xia, Z. Design principles for covalent organic frameworks as efficient electrocatalysts in clean energy conversion and green oxidizer production. *Adv. Mater.* **2017**, *29*, 1606635.
(41) Solovyev, I. V.; Dederichs, P. H.; Anisimov, V. I. Corrected atomic limit in the local-density approximation and the electronic structure of d impurities in Rb. *Phys. Rev. B* **1994**, *50*, 16861.
(42) Cheng, D.; Cao, D.; Zeng, X. C. Personal Communication.
(43) Lin, S.; Xu, H.; Wang, Y.; Zeng, X. C.; Chen, Z. Directly predicting limiting potentials from easily obtainable physical properties of graphene-supported single-atom electrocatalysts by machine learning. *J. Mater. Chem. A* **2020**, *8*, 5663−5670.
(44) Samantaray, M. K.; D'Elia, V.; Pump, E.; Falivene, L.; Harb, M.; Ould Chikh, S.; Cavallo, L.; Basset, J.-M. The Comparison between Single Atom Catalysis and Surface Organometallic Catalysis. *Chem. Rev.* **2020**, *120* (2), 734−813.
(45) De Rita, L.; Resasco, J.; Dai, S.; Boubnov, A.; Thang, H. V.; Hoffman, A. S.; Ro, I.; Graham, G. W.; Bare, S. R.; Pacchioni, G.; Pan, X.; Christopher, C. Structural evolution of atomically dispersed Pt catalysts dictates reactivity. *Nat. Mater.* **2019**, *18*, 746−751.
(46) Tang, Y.; Asokan, C.; Xu, M.; Graham, G. W.; Pan, X.; Christopher, P.; Li, J.; Sautet, P. Rh single atoms on TiO_2 dynamically respond to reaction conditions by adapting their site. *Nature Commun.* **2019**, *10*, 1−10.
(47) Mennucci, B.; Cances, E.; Tomasi, J. Evaluation of solvent effects in isotropic and anisotropic dielectrics and in ionic solutions with a unified integral equation method: theoretical bases, computa-

https://doi.org/10.1021/acscatal.2c01011
ACS Catal. 2022, 12, 5846−5856

tional implementation, and numerical applications. *J. Phys. Chem. B* **1997**, *101*, 10506−10517.
(48) Ishikawa, Y.; Mateo, J. J.; Tryk, D. A.; Cabrera, C. R. Direct molecular dynamics and density-functional theoretical study of the electrochemical hydrogen oxidation reaction and underpotential deposition of H on Pt(111). *J. Electroanalyt. Chem.* **2007**, *607*, 37−46.
(49) Gauthier, J. A.; Dickens, C. F.; Chen, L. D.; Doyle, A. D.; Nørskov, J. K. Solvation effects for oxygen evolution reaction catalysis on IrO_2 (110). *J. Phys. Chem. C* **2017**, *121*, 11455−11463.
(50) Tang, M. T.; Liu, X.; Ji, Y.; Nørskov, J. K.; Chan, K. Modeling hydrogen evolution reaction kinetics through explicit water-metal interfaces. *J. Phys. Chem. C* **2020**, *124*, 28083−28092.
(51) Calle-Vallejo, F.; de Morais, R.; Illas, F.; Loffreda, D.; Sautet, P. Affordable estimation of solvation contributions to the adsorption energies of oxygenates on metal nanoparticles. *J. Phys. Chem. C* **2019**, *123*, 5578−5582.
(52) Iyemperumal, S. K.; Deskins, N. A. Evaluating solvent effects at the aqueous/Pt (111) interface. *ChemPhysChem* **2017**, *18*, 2171−2190.
(53) Yang, G.; Akhade, S. A.; Chen, X.; Liu, Y.; Lee, M. S.; Glezakou, V. A.; Rousseau, R.; Lercher, J. A. The nature of hydrogen adsorption on platinum in the aqueous phase. *Angew. Chem., Int. Ed.* **2019**, *58*, 3527−3532.
(54) Wang, J.; Chang, K.; Sun, Z.; Lee, J. H.; Tackett, B. M.; Zhang, C.; Chen, J. G.; Liu, C. J. A Combined experimental and theoretical study of the accelerated hydrogen evolution kinetics over wide pH range on porous transition metal doped tungsten phosphide electrocatalysts. *Appl. Catal. B: Environ.* **2019**, *251*, 162−167.
(55) Dubouis, N.; Grimaud, A. The hydrogen evolution reaction: from material to interfacial descriptors. *Chem. Sci.* **2019**, *10*, 9165−9181.
(56) Liu, T.; Li, P.; Yao, N.; Cheng, G.; Chen, S.; Luo, W.; Yin, Y. CoP-doped MOF-based electrocatalyst for pH-universal hydrogen evolution reaction. *Angew. Chem.* **2019**, *131*, 4727−4732.
(57) Men, Y.; Li, P.; Yang, F.; Cheng, G.; Chen, S.; Luo, W. Nitrogen-doped CoP as robust electrocatalyst for high-efficiency pH-universal hydrogen evolution reaction. *Appl. Catal. B: Environ.* **2019**, *253*, 21−27.
(58) Valdés, Á.; Qu, Z. W.; Kroes, G. J.; Rossmeisl, J.; Nørskov, J. K. Oxidation and photo-oxidation of water on TiO_2 surface. *J. Phys. Chem. C* **2008**, *112*, 9872−9879.
(59) Exner, K. S. Paradigm change in hydrogen electrocatalysis: The volcano's apex is located at weak bonding of the reaction intermediate. *Inter. J. Hydrog. En.* **2020**, *45*, 27221−27229.
(60) Lindgren, P.; Kastlunger, G.; Peterson, A. A. A challenge to the G∼ 0 interpretation of hydrogen evolution. *ACS Catal.* **2020**, *10*, 121−128.
(61) Ooka, H.; Nakamura, R. Shift of the optimum binding energy at higher rates of catalysis. *J. Phys. Chem. Lett.* **2019**, *10*, 6706−6713.
(62) Li, X.; Rong, H.; Zhang, J.; Wang, D.; Li, Y. Modulating the local coordination environment of single-atom catalysts for enhanced catalytic performance. *Nano Res.* **2020**, *13*, 1842−1855.
(63) Zhang, J.; Yang, H.; Liu, B. Coordination engineering of single-atom catalysts for the oxygen reduction reaction: a review. *Adv. Ener. Mater.* **2021**, *11*, 2002473.
(64) Zhang, T.; Walsh, A. G.; Yu, J.; Zhang, P. Single-atom alloy catalysts: structural analysis, electronic properties and catalytic activities. *Chem. Soc. Rev.* **2021**, *50*, 569−588.
(65) Fei, H.; Dong, J.; Chen, D.; Hu, T.; Duan, X.; Shakir, I.; Huang, Y.; Duan, X. Single atom electrocatalysts supported on graphene or graphene-like carbons. *Chem. Soc. Rev.* **2019**, *48*, 5207−5241.
(66) Thang, H. V.; Pacchioni, G.; De Rita, L.; Christopher, P. Nature of stable single atom Pt catalysts dispersed on anatase TiO_2. *J. Catal.* **2018**, *367*, 104−114.
(67) Fei, H.; Dong, J.; Arellano-Jiménez, M. J.; Ye, G.; Dong Kim, N.; Samuel, E. L. G.; Peng, Z.; Zhu, Z.; Qin, F.; Bao, J.; Yacaman, M. J.; Ajayan, P. M.; Chen, D.; Tour, J. M. Atomic Cobalt on Nitrogen-Doped Graphene for Hydrogen Generation. *Nat. Commun.* **2015**, *6* (1), 8668.
(68) Qiao, W.; Xu, W.; Xu, X.; Wu, L.; Yan, S.; Wang, D. Construction of Active Orbital via Single-Atom Cobalt Anchoring on the Surface of 1T-MoS_2 Basal Plane toward Efficient Hydrogen Evolution. *ACS Appl. Energy Mater.* **2020**, *3* (3), 2315−2322.
(69) Zhang, L.; Jia, Y.; Gao, G.; Yan, X.; Chen, N.; Chen, J.; Soo, M. T.; Wood, B.; Yang, D.; Du, A.; Yao, X. Graphene Defects Trap Atomic Ni Species for Hydrogen and Oxygen Evolution Reactions. *Chem.* **2018**, *4* (2), 285−297.
(70) Li, X.; Yang, X.; Zhang, J.; Huang, Y.; Liu, B. In situ/operando techniques for characterization of single-atom catalysts. *ACS Catal.* **2019**, *9*, 2521−2531.
(71) Li, K.; Wang, X.; Zhang, F.; Xue, D. Electronegativity identification of novel superhard materials. *Phys. Rev. Lett.* **2008**, *100*, 235504.
(72) Walsh, A.; Sokol, A. A.; Buckeridge, J.; Scanlon, D. O.; Catlow, C. R. A. Oxidation states and ionicity. *Nat. Mater.* **2018**, *17*, 958−964.
(73) Cao, B.; Hu, M.; Cheng, Y.; Jing, P.; Liu, B.; Zhou, B.; Wang, X.; Gao, R.; Sun, X.; Du, Y.; Zhang, J. Tailoring the d-band center of N-doped carbon nanotube arrays with Co_4N nanoparticles and single-atom Co for a superior hydrogen evolution reaction. *NPG Asia Mater.* **2021**, *13*, 1−14.
(74) Hammer, B.; Morikawa, Y.; Nørskov, J. K. CO chemisorption at metal surfaces and overlayers. *Phys. Rev. Lett.* **1996**, *76*, 2141−2144.
(75) Hoffmann, R. How chemistry and physics meet in the solid state. *Angew. Chem., Int. Ed. Engl.* **1987**, *26*, 846−878.
(76) Zafari, M.; Kumar, D.; Umer, M.; Kim, K. S. Machine learning-based high throughput screening for nitrogen fixation on boron-doped single atom catalysts. *J. Mater. Chem. A* **2020**, *8*, 5209−5216.
(77) Pablo-García, S.; Sabadell-Rendón, A.; Saadun, A. J.; Morandi, S.; Pérez-Ramírez, J.; López, N. Generalizing Performance Equations in Heterogeneous Catalysis from Hybrid Data and Statistical Learning. *ACS Catal.* **2022**, *12*, 1581−1594.

https://doi.org/10.1021/acscatal.2c01011
ACS Catal. 2022, 12, 5846−5856